Segregation of Fluidized Binary Mixtures of Granular Solids

Giuseppe Olivieri, Antonio Marzocchella, and Piero Salatino
Dipartimento di Ingegneria Chimica, School of Engineering/School of Biotechnological Science, Università degli Studi di Napoli Federico II, 80125 Naples, Italy

DOI 10.1002/aic.10340
Published online in Wiley InterScience (www.interscience.wiley.com).

Fluidization behavior of binary mixtures of solids is addressed. Three binary systems were considered, obtained by mixing monodisperse granular solids of different size and/or density. A segmented fluidization column equipped with multiple pressure transducers was the experimental apparatus. Monitoring of pressure at different locations along the bed and direct characterization of solids contained in each segment were the experimental tools. The binary granular beds were in one of the following states, depending on gas superficial velocity and initial mixture fraction: fixed, bubbly-free fluidization, transient fluidization, and bubbling steady fluidization. Fluidization regimes were mapped in a gas superficial velocity vs. initial mixture fraction phase plane. Axial solids concentration profiles along the bed and solids segregation rates were also assessed for the three systems as a function of the operating conditions of the bed. Differences and similarities between the systems were analyzed and interpreted in the light of the basic segregation patterns. In particular whether a defluidized bottom layer of jetsam-rich solids is formed upon segregation appears to be an important key to the segregation phenomenology. The currently available models for the prediction of solids segregation in fluidized beds prove to be helpful to understand the qualitative features of the phenomenology, but fall short when quantitative prediction of segregation parameters is afforded. © 2004 American Institute of Chemical Engineers *AIChE J,* 50: 3095–3106, 2004
Keywords: fluidization, solids mixture, mixing/segregation, mixing index, drift flux

Introduction

Fluidization of beds of dissimilar particles is closely associated with possible occurrence of segregation phenomena that result into uneven distribution of solid classes within the bed. Depending on the relevant application,[1-6] particle segregation can be regarded as either an undesired phenomenon to be prevented or a process to be emphasized, as in classifiers of polydisperse granular mixtures. In either case careful characterization of the extent and dynamics of particle segregation is an essential prerequisite for the proper design and operation of fluidized bed units.

Correspondence concerning this article should be addressed to A. Marzocchella at antonio.marzocchella@unina.it.

Experimental studies on fluidization of beds of dissimilar solids mostly concerned the onset of the fluidized state and the distribution of solids throughout the bed.[2,7-14] To a lesser extent, the dynamics of segregation phenomena was addressed.[2,7,15-22] Despite the extensive literature regarding mixing/segregation in aerated/fluidized beds of dissimilar solids, comprehensive understanding of fluidization regimes and of the dynamics of segregation phenomena is still lacking.

Gibilaro and Rowe[23] analyzed mixing/segregation during fluidization of polydisperse solids from a mechanistic perspective. They developed a model for the prediction of solids concentration profiles establishing at steady state along the bed. Since then, other models have been proposed to predict the extent of segregation in steadily fluidized beds, based either on the Gibilaro and Rowe concept[11,24-26] or on different ones.[7,15,27] The dynamical features of solids segregation have also been

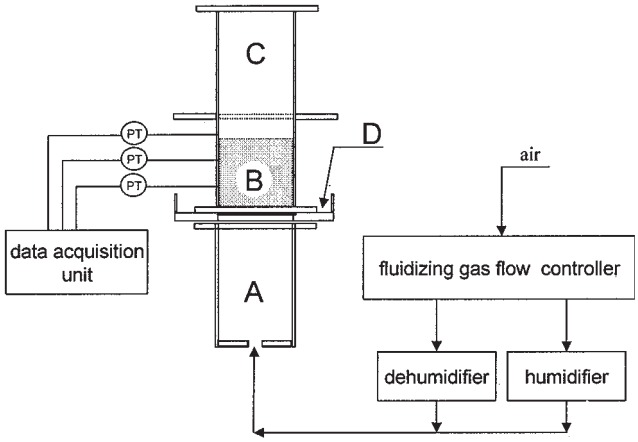

Figure 1. Experimental apparatus.

(A) windbox; (B) fluidized bed; (C) freeboard; (D) solids collection plate. PT, pressure transducer.

modeled, either following the Gibilaro and Rowe mechanistic framework[26,28] or through CFD-based approaches.[29-31] Even though dynamical and steady-state models available in literature can effectively reproduce the basic features of the phenomenology, quantitative predictions are still critically dependent on experiment-based assessment of parameters. Unknown parameters may regard the behavior of particles ensembles (such as collisions parameters) or the flow structures of the binary solids suspension (bubble diameter, bubble wake fraction, bubble velocity).[11,15,24,25,29]

Marzocchella et al.[32,33] recently reported experimental results regarding the fluidization behavior of beds of dissimilar solids characterized by equal density and different size. The following features were specifically addressed: (1) the hydrodynamic regime that establishes in a bed as a function of superficial gas velocity and solids mixture composition; (2) the unsteady state of fluidization that may establish at gas superficial velocity below the threshold for the complete and uniform fluidization of solids mixtures; (3) the dynamics of particle segregation, expressed through the drift flux velocity of the mixture components. Three fluidization regimes were identified in a mixture concentration-gas superficial velocity phase plane: fixed bed, at low velocity; steadily fluidized bed, at large velocity; transient fluidization, in an intermediate velocity range. The distinctive feature of the latter regime, in agreement with findings of Hoffmann et al.,[11] is that an initially uniform fluidized bed eventually undergoes segregation, giving rise to a defluidized bottom layer rich in the coarser solids and to a "supernatant" fluidized layer where finer particles prevail. The rates at which the defluidized solids layer builds up from initially uniform beds and the ultimate compositions of the defluidized bottom and fluidized top layers were reported by Marzocchella et al.[33]

The present work moves one step further along the direction of characterizing the extent and rate of solids segregation in beds of polydisperse solids. The experimental approach of Marzocchella et al.[33] is extended to a spectrum of binary granular mixtures characterized by different combinations of size and/or densities. Regions within which the fixed-bed state, the steadily fluidized state, and transient fluidization establish are mapped in the mixture concentration-gas superficial velocity phase plane. The dynamical features of segregation of beds of dissimilar solids are also analyzed.

Experimental

Apparatus

The experimental apparatus, shown in Figure 1, consists of a 0.12-m ID Plexiglas fluidization column, 1.5 m high, equipped with a gas flow controller, a dehumidifier, a humidifier, a set of electronic pressure transducers, and a data-acquisition unit.[34] The lower part of the column consists of an assembly of cylindrical segments, each 2.5 cm high, and equipped with a pressure tap connected to a transducer. The fluidizing gas is fed through a sintered brass distributor characterized by a high pressure drop. The dehumidifier consists of a fixed bed of silica gel high enough to bring humidity in the fluidizing gas to less than 5%, as measured by a digital hygrometer. The humidifier consisted of a water bubble column with a droplet disengagement zone. Pressure transducers were of high-precision piezoelectric type. The data-acquisition unit consists of a PC equipped with a 12 A/D data acquisition board. Pressure time series were logged on at preset sampling frequencies (100–200 Hz) and for fixed time intervals (0.5–20 min).

Materials

Table 1 reports the main properties of the granular solids used in the investigation. Table 2 reports the two binary mixtures that were specifically investigated in the present study, and a third mixture, previously investigated,[33] was also considered, as follows:

(1) System 1: 125 μm silica sand; 375 μm silica gel
(2) System 2: 500 μm silica sand; 500 μm polypropylene
(3) System 3: 500 μm glass beads; 125 μm silica sand

The three systems were selected so as to be representative of broadly different fluidization patterns of binary mixtures. Table

Table 1. Properties of Granular Solids Investigated

Acronym	SS-I	SS-II	SG	PP	GB
Material	Silica sand	Silica sand	Silica gel	Polypropylene	Glass
Sauter mean diameter, μm	125	500	375	500	500
Size range, μm	100–150	400–600	350–400	400–600	400–600
Sphericity	$\approx$1	$\approx$1	$\approx$1	$\approx$1	1
Particle density, kg/m^3	2600	2600	600	900	2540
Geldart group	B	B	A-B	B	B
Minimum fluidization velocity, m/s	2.2×10^{-2}	1.9×10^{-1}	3.2×10^{-2}	1.1×10^{-1}	2.3×10^{-1}
Terminal velocity,* m/s	0.80	4.1	1.25	1.42	4.1

*Value calculated according to Haider and Levenspiel.[35]

Table 2. Properties of Binary Solid Mixtures Investigated

System	Solids (Notation as in Table 1)		Comparison of:		
	Jetsam	Flotsam	Density	Size	Incipient Fluidization Velocity
1	SS-I	SG	$\rho_J/\rho_F \cong 4$	$d_J/d_F \cong 0.3$	$U_{mf,J} \cong 2U_{mf,F}$
2	SS-II	PP	$\rho_J/\rho_F \cong 3$	$d_J/d_F = 1$	$U_{mf,J} \cong 0.5U_{mf,F}$
3*	GB	SS-I	$\rho_J/\rho_F = 1$	$d_J/d_F \cong 0.3$	$U_{mf,J} \cong 13U_{mf,F}$

*After Marzocchella et al.[33]

2 indicates how particle size, particle density, and incipient fluidization velocity of the individual components compare with each other. System 1 is characterized by components differing in both density and size in a way that incipient fluidization velocity is within a factor of 2. It is noteworthy that $U_{mf,J} < U_{mf,F}$ in this case, consistent with the known feature that density differences frequently overtake size differences as the driving force of segregation.[36] System 2 is characterized by solids components having equal diameters and different densities. Again, denser particles are the jetsam in this case.[36] System 3 is characterized by solids components having equal densities and different particle sizes. Coarser particles represent the jetsam component.[36] In any case, solids were chosen with the further constraint that the terminal velocity of the flotsam be larger than the minimum fluidization velocity of the jetsam.

Bed inventory was chosen so as to operate with an aspect ratio (height/diameter) of the fixed homogenously mixed bed of about 1.1–1.2 (bed height ranging between 13.2 and 14.4 cm).

The fluidizing gas was technical air split into two streams: the first was sent to the dehumidifier and the second to the humidifier. Mixing of these two streams at fixed proportion served the purpose of controlling the relative humidity in the range from dry to saturated. The humidity level was optimized for each mixture to prevent noneven fluidization, considering the twofold effect of humidity on interparticle forces: increasing humidity enhances capillary forces, especially for nonporous materials,[37] whereas it prevents the onset of triboelectrostatic forces. Despite careful optimization of the procedure, electrostatic charging of polypropylene particles could not be fully prevented in experiments with System 2.

Procedures

Experimental procedures were slightly different, depending on whether System 1 or System 2 mixtures were used.

System 1. The bed preparation procedure conformed to that used by Marzocchella et al.[33]: bed solids were kept in an oven at 110–120°C for 1 h to remove moisture; solids were mixed in the desired proportion in a rotary mixer for 1 h, after which the bed material was gently poured into the column.

System 2. Solids were gently dried in an oven, then mixed in the desired proportion and poured into the column. Mixing in the rotary mixer could not be accomplished because of extensive electrostatic charging. The alternative mixing procedure was adopted, consisting of fluidizing the bed under vigorous bubbling regime for about 30 min, then shutting off the fluidizing gas.

Both System 1 and System 2 mixtures were subjected to two types of experiments:

Type A. Gas superficial velocity U was quasi-steadily increased starting from the fixed bed state until the bed became fully fluidized. Then, the superficial gas velocity was slowly reduced until the bed returned into the fixed state.

Type B. Gas superficial velocity was suddenly raised from zero to a preset value, and the bed was kept fluidized for times ranging from 0.5 to 20 min. After the preset fluidization time expired the bed was "frozen" by suddenly shutting the fluidizing gas flow off.

In both types of experiments, gas pressure (P) at different levels in the bed was continuously recorded. In some cases size distributions of solids in each segment were directly obtained at the end of experiments. To this end, cylindrical segments were disassembled one at a time, gently pouring the bed solids contained therein into the collection plate D (Figure 1) from which they were further retrieved for subsequent analysis.

The characterization of mixture composition was accomplished using two methods: solids sieving was adopted for System 1; sink-float gravity classification in water (with polypropylene floating) was adopted for System 2.

The axial profile of the solids mixture fraction X_J along the bed could be determined accordingly. X_J was defined as the volumetric fraction of the jetsam with respect to the solids mixture, not including interparticle voidage. The control volumes over which X_J could be measured were those of the cylindrical segments (ID 12.0 cm, height 2.5 cm). Therefore, they represented averages over each segment.

Solids mixture fraction profiles were eventually worked out to estimate a mixing index, M[33]

$$M = \frac{\int_0^{H^*} |X_J^* - X_J| dz}{\int_0^{H^*} |X_J^* - X_{J0}| dz} \tag{1}$$

where H^* is the static bed height in the completely segregated state. According to the definition, M is a measure of the deviation between the actual solids composition profile and that associated with the completely segregated state $X_J^*(z)$: jetsam particles segregated at the bed bottom ($X_J^*=1$) and flotsam particles at the top ($X_J^*=0$). The index M, normalized with respect to the condition of completely mixed state ($X_J = X_{J0}$ throughout the bed), ranges between 0 and 1, corresponding to completely segregated and to well-mixed beds, respectively.

A few experiments were purposely carried out in which axial solids concentration profiles were assessed to check the bed mixing state before fluidization experiments began. Mixture composition was measured immediately after charging the bed,

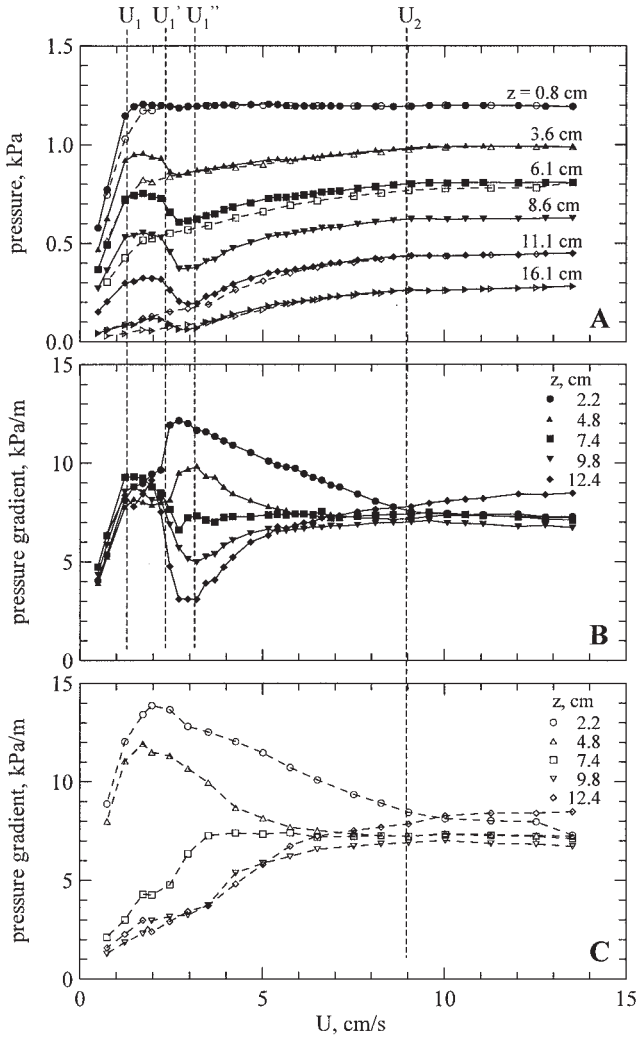

Figure 2. Pressure (A) and pressure gradient (B and C) as functions of gas superficial velocity at different tap locations.

System 1-mixtures. Average jetsam volumetric fraction = 0.5. Closed symbols: increasing U; hollow symbols: decreasing U.

in the case of experiments with System 1, or just after the prestirring by vigorous fluidization that followed charging of the bed, in the case of experiments with System 2. No appreciable segregation was found before the beginning of either type A or type B experiments with both kind of mixtures.

Local bed density (ρ_b) under fluidized conditions was calculated as $\rho_b = \Delta P/(g\,\Delta z)$, where g is the acceleration attributed to the gravity and Δz is the distance between pressure taps. For particles of equal density (ρ_s), the voidage (ε) can be evaluated as $\varepsilon = 1 - (\rho_b/\rho_s)$.

Results

System 1

Figure 2 reports results of a type A experiment carried out using a silica sand–silica gel (System 1) mixture characterized by jetsam volumetric fraction of 50% (bed weight = 2850 g). The pressure (Figure 2A) and the pressure gradients at both increasing (Figure 2B) and decreasing (Figure 2C) values of the gas superficial velocity (U) at different levels across the bed are reported.

As the gas superficial velocity is increased quasi-steadily during a type A experiment, the following sequence of states and transitions is observed:

(1) $U < U_1 \cong 1.5$ cm/s. The solids are in the fixed-bed state. The pressure measured at the bed bottom ($z = 0.6$ cm) increases until it reaches the value corresponding to the bed weight per unit cross-sectional area ($W_{bed}/A \cong 1.2$ kPa) at $U \cong U_1$. The pressure gradient is constant throughout the bed and increases with U.

(2) $U_1 < U < U_1' \cong 2.2$ cm/s. The fluidized bed expands homogeneously (bubble-free fluidization regime). The pressure measured along the bed is approximately constant with U. Bed voidage increases with U. Correspondingly, a slight decrease of the pressure drop is recorded.

(3) $U_1' < U < U_2 = 9.1$ cm/s. Bubbles become apparent and segregation of sand particles at the bed bottom starts. The pressure at the bed bottom is approximately constant, whereas that measured at higher pressure taps decreases as a result of the progressive increase of silica-gel (low density) particles concentration in the upper region. Notably, the occurrence of particle segregation is very well highlighted by the pressure gradient that: (i) approaches a value corresponding to bulk bed density of about 1200 kg/m^3 in the lower region of the bed, close to the value measured in a fluidized bed of sand; (ii) approaches values close to that typical of a fluidized bed of pure silica gel in the upper region of the bed. Solids segregation is extensive at $U = U_1''$. Increasing U even further, bubble-induced mixing progressively overtakes segregation until the bed becomes uniform. The pressure gradients tend to a uniform value throughout the bed.

(4) $U_2 < U$. Vigorous bubbling establishes in a bed of fairly uniform composition.

By decreasing the superficial gas velocity quasi-steadily it is noted that (Figure 2C):

(1) $U < U_2$. Sand particles segregate at the bottom, yielding a high-density fluidized bed. Correspondingly, gel particles segregate at the surface, yielding a low-density fluidized bed. Particle separation progressively extends to inner regions of the bed, and only at $U < 5$–6 cm/s does it affect the bed region between 5.9 and 9.9 cm. A constant value of bed density is approached in each layer of the bed.

(2) $U < 2$ cm/s. Pressure at the bed bottom and pressure drop across the bed decrease. The bed is in the fixed-bed regime.

It should be noted that the "inverted" fluidization pattern recognized by Rasul et al.[12] and van Wachem et al.[30] in beds of dissimilar solids resembling System 1 was not observed in the present study. It is likely that larger gas superficial velocities might be necessary to establish this singular fluidization pattern.

It is interesting to note that particulate fluidization is observed in the velocity range $U_1 < U < U_1'$, even though each of the two components of the mixture alone behaves as a B-group solid of the Geldart classification of powders. It is likely that delayed bubbling is a consequence of the enhancement of interparticle forces attributed to the presence of smaller particles in the spacings between coarser ones. The increased contact point density between particles associated with size

polydispersity might affect the importance of attractive forces[38,39] as well as of interparticle forces of frictional nature.

Hysteresis observed in pressure profiles is typical of the fluidization curve of solids with broad particle size distribution.[2] However, in the present case it regards the pressure gradient as well. As U is decreased, segregation yields two layers laid one on top of the other: a sand-rich bottom fluidized bed and a gel-rich top bed. Bulk density of these layers is close to that of fluidized beds of either component alone ($\cong$1300 kg/m^3 for the bed of sand and $\cong$300 kg/m^3 for the bed of gel). Direct observation of the bed supports these findings: a white layer of silica gel becomes apparent at the top of the bed, whereas a brown layer of silica sand becomes apparent at the bottom. As expected, the bubble-free expanded bed state is not observed as U is decreased: even in the range of gas superficial velocities $U_1 < U < U_1'$, the bed is in the bubbling state. It is likely that the persistence of bubbling at U close to U_1 emphasizes particle segregation as U is decreased when compared with the extent of segregation correspondingly observed as U is increased.

It may be noted in Figure 2C that the "supernatant" silica gel bed establishes at superficial velocities even smaller than the minimum fluidization velocity of the silica-gel flotsam particles ($U_{mf,F}$ = 3.2 cm/s). Under these operating conditions, and over a limited range of gas superficial velocities, a singular phenomenon is observed: a fixed-bed layer establishes at the top, intermittently disturbed by bubbles rising from the underneath sand-rich fluidized bed. The fixed bed of silica gel is locally and occasionally fluidized (or one should rather say, shaken) by the gas present in bubbles, which vanish as they rise across the layer. This phenomenon becomes progressively less evident as the gas superficial velocity decreases and disappears at $U < 2$ cm/s.

The same general behavior was observed using System 1 mixtures of different initial jetsam concentration X_{J0}, ranging between 0 and 1. Figure 3.1 reports the average bed voidage of thoroughly mixed fixed beds of System 1 mixtures of different concentrations. In the same figure the bed voidage of fluidized beds on the verge of bubbling ($U = U_1'$) is reported. The minimum of fixed-bed voidage found at $X_{J0} \cong 0.3$ is typical of binary mixtures of particles of different size.[10,40] The bed voidage at the onset of bubbling is practically constant with X_{J0} and, as expected, particulate fluidization does not establish at any gas superficial velocity when fluidizing single-component beds.

Figure 4.1 summarizes results obtained with type A experiments using System 1 mixtures: gas superficial velocities corresponding to regime transitions are mapped as functions of the initial volumetric concentration of the jetsam component, X_{J0}. U_1 and U_1' are scarcely affected by X_{J0}; U_2 presents a pronounced maximum at about X_{J0} = 10%.

Type B experiments aimed at assessing the dynamics and the ultimate extent of segregation at different values of the gas superficial velocity in the interval between U_1 and U_2. Figure 5 reports typical time-resolved pressure profiles measured during a run in which fluidization was suddenly established by a stepwise change of gas superficial velocity from 0 to 3.2 cm/s. The bed consisted of a System 1 mixture with X_{J0} = 0.20. Pressure measured at the bed bottom (z = 0.8 cm) increases sharply up to a value corresponding to the bed weight per unit cross-sectional area, indicating that the whole bed is completely fluidized during the experiment. Similarly, pressures measured at higher levels suddenly jump to values corresponding to the initial bed mass present above the measurement levels, after which they decay toward asymptotic steady values, consistent with the decrease of the mass of solids above the pressure taps. It is inferred that this is a consequence of segregation of sand at the bed bottom and, conversely, of silica gel to the top of the bed.

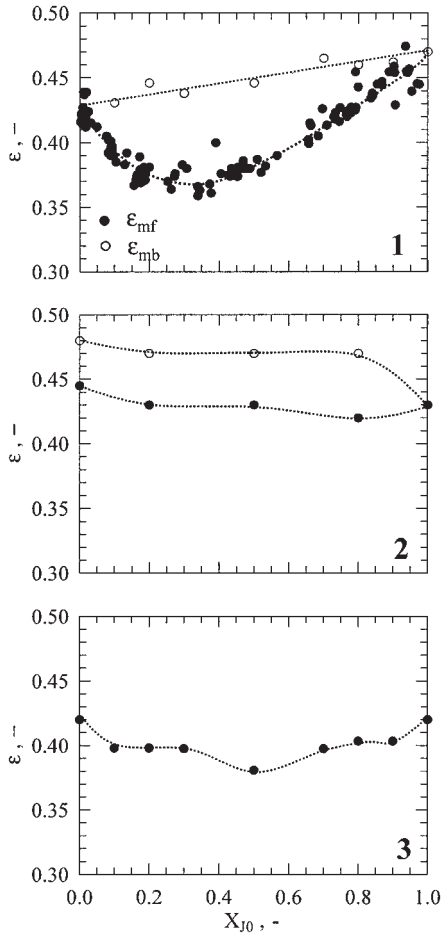

Figure 3. Average voidage of mixtures under well-mixed settled bed (●) and at the onset of transient fluidization regime (○) as functions of the average volumetric jetsam fraction.

(1) System 1; (2) System 2; (3) System 3.

Axial profiles of jetsam concentration X_J have been estimated at the end of type B experiments at gas superficial velocities $U_1(X_{J0}) < U < U_2(X_{J0})$. Profiles obtained at the end of experiments lasting different times were compared. It appears that steady profiles are approached when the fluidization time is longer than 2 min. Ultimate profiles of X_J are reported in Figure 6 for runs carried out with solids mixtures having X_{J0} = 0.2. Data are qualitatively similar to those obtained by previous investigators using different techniques.[2,7,11,17] Jetsam concentration is uniform and equal to X_{J0} throughout the bed at $U_1(X_{J0}) < U < U_1'(X_{J0})$. The bed is almost completely segregated at U just above U_1', then the degree of segregation decreases as gas velocity is increased from U_1' to U_2 (16.5 cm/s). Segregation phenomena are significant at U close to U_1'

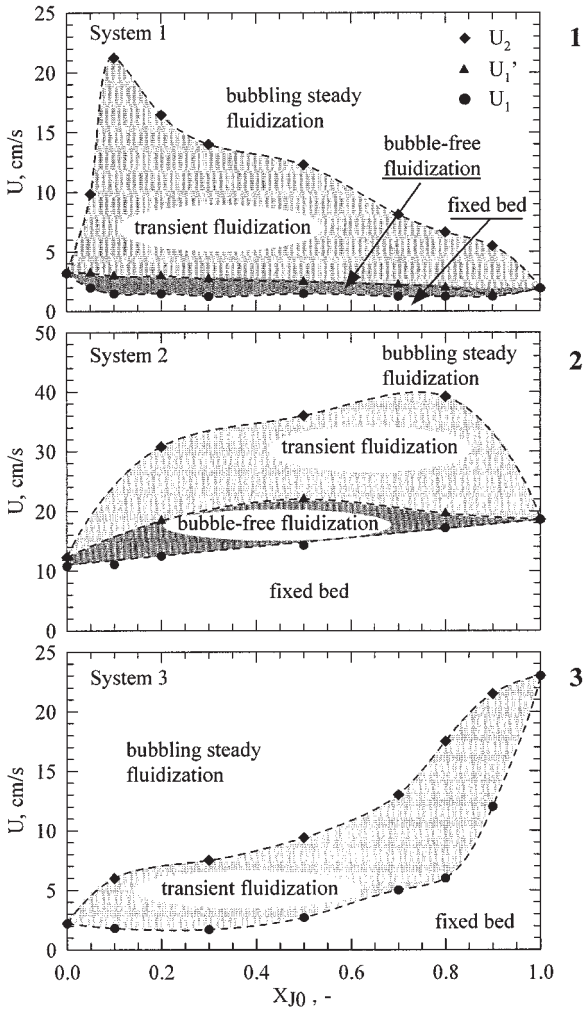

Figure 4. Transition gas superficial velocities between fluidization regimes as functions of X_{J0} for System 1, System 2, and System 3 (after Marzocchella et al.[33]).

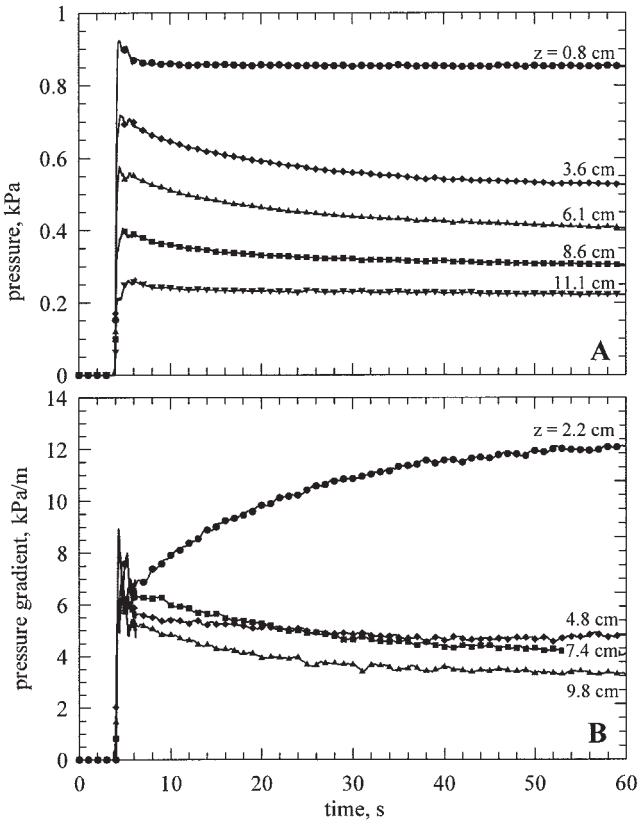

Figure 5. Time-resolved pressure profiles (A) and pressure gradient profiles (B).

System 1: $X_{J0} = 0.20$. $U = 3.19$ cm/s.

and the bed is split into fully segregated layers of either pure jetsam ($X_J = 1$) or flotsam ($X_J = 0$). Profiles qualitatively similar to those in Figure 6 were measured with solids mixtures characterized by X_{J0} in the range between 0.1 and 0.8.

Axial solids concentration profiles have been worked out to estimate the mixing index M according to Eq. 1. Figure 7.1 reports M as a function of the gas superficial velocity for each X_{J0} investigated. The mixing index is 1 for $U < U'_1$. It suddenly drops as soon as U departs from U'_1, then it approaches 1 when U increases, that is, when mixing phenomena overcome segregation.

Analysis of axial solid concentration profiles (like those in Figure 6) suggested that the System 1 mixtures, either partly or fully segregated, conformed reasonably well to the simplified assumption consisting of considering the bed as two layered zones at relatively uniform jetsam volumetric fractions: X_{JT} in the top layer and X_{JB} in the bottom layer. Experimental values of X_{JB} and X_{JT} are reported in Figure 8.1 as functions of U and of the initial volumetric fraction of the jetsam component X_{J0}. It can be noted that in the range of U between U'_1 and U_2 and for any X_{J0}, data points are fairly aligned along two loci: the left locus corresponds to the composition of the top layer X_{JT}; the right locus corresponds to the composition of the bottom layer X_{JB}. As U approaches U_2, solids composition of the two fluidized layers converge toward the average value X_{J0}, indi-

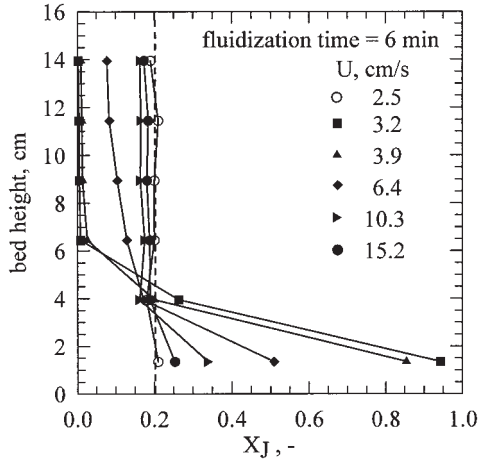

Figure 6. Axial profiles of solids concentration measured after fluidization for 6 min at different gas superficial velocities.

System 1: $X_{J0} = 0.2$.

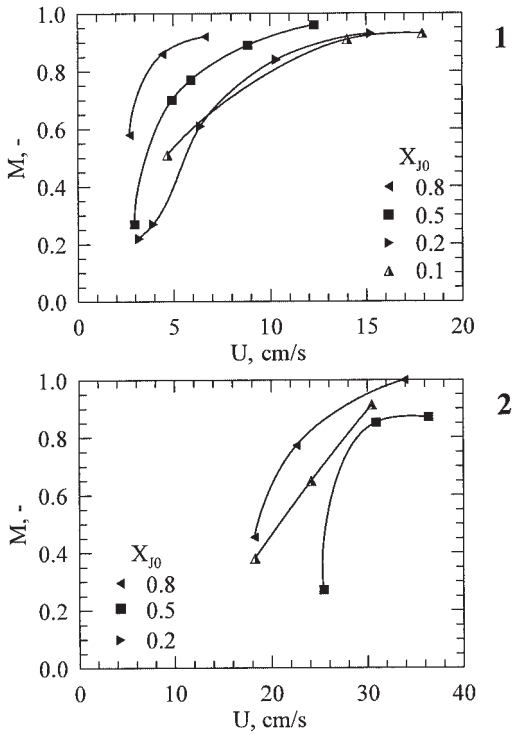

Figure 7. Mixing index as a function of superficial velocity after 6 min fluidization.

B-type experiments for different values of X_{J0}. (1) System 1; (2) System 2.

cating that bubble-promoted mixing overcomes segregation at these velocities.

Pressure time series recorded during type B experiments at variables U and X_{J0} were worked out, as detailed in the Appendix, to calculate the drift flux velocity J_{Jm}. Averages over data obtained at different pressure measurement levels were calculated and are mapped in Figure 9.1. The drift flux velocity reaches a maximum at U close to $U = U'_1(X_{J0})$, to decrease toward vanishingly small values as U approaches $U_2(X_{J0})$. The closer U is to U_2, the smaller the extent of solids segregation. This makes the determination of the pressure derivative $\partial P/\partial t$ and of the associated value of J_{Jm} increasingly difficult as U_2 is approached.

System 2

Characterization of System 2 mixtures for different initial mixture fractions X_{J0} has been carried out using the basic procedure followed for System 1.

Typical results of type A experiments with a System 2 mixture of initial jetsam volumetric fraction $X_{J0} = 0.50$ are shown in Figure 10. Pressure (Figure 10A) and pressure gradients (Figures 10B and C) measured at different levels in the bed are reported as functions of gas superficial velocity. Figure 10B refers to measurements carried out at increasing velocity and Figure 10C at decreasing velocity. Velocities U_1, U'_1, and U_2 can be identified as thresholds between fixed-bed, bubble-free fluidization, transient fluidization, and steady fluidization of the mixtures similarly to System 1 mixtures.

The general phenomenology resembles that observed in experiments with System 1 mixtures: (i) the denser solid component behaves as jetsam; (ii) hysteresis in the fluidization curve at increasing/decreasing gas superficial velocity is observed, and (iii) jetsam segregation is far more pronounced during runs carried out at decreasing gas superficial velocity. However, Figure 10C shows that in the upper part of the bed the bulk density of the suspension ($\cong$700 kg/m^3) is greater than that of polypropylene fluidized bed (about 500 kg/m^3). The upper layer consists of a polypropylene–sand mixture at lower jetsam concentration with respect to the average value X_{J0}.

Measurements carried out decreasing U indicate that at $U < U_{mf,J} = 17$ cm/s a sand-rich fixed bed establishes at the bottom with the formation of a polypropylene-rich supernatant fluidized bed.

The same general behavior was found when the sand volumetric fraction X_{J0} in the mixture was changed between zero and one. The average bed voidage of the initially settled

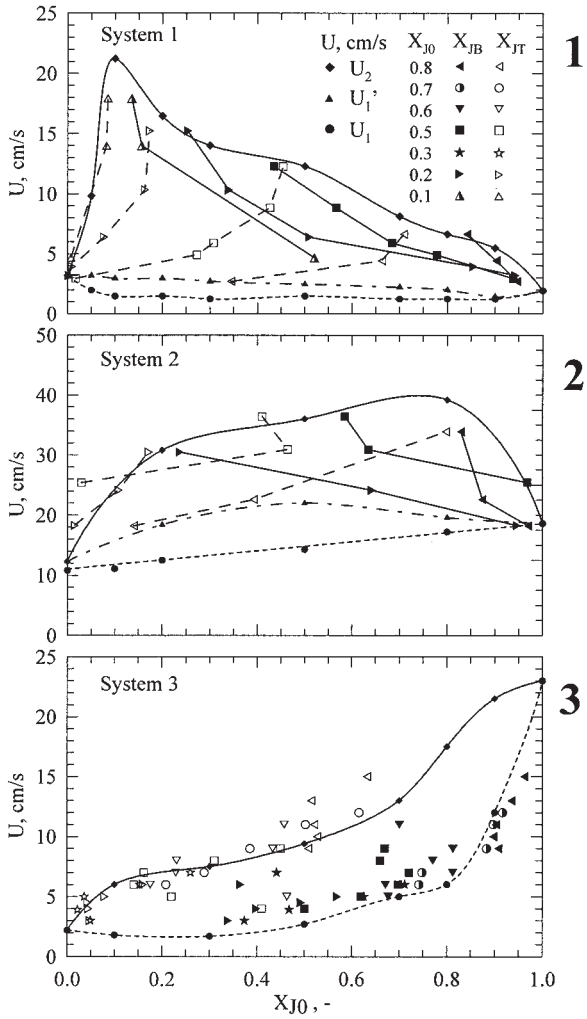

Figure 8. Loci of the jetsam volume fractions in the top (X_{JT}) and in the bottom (X_{JB}) fluidized layer as functions of gas superficial velocities for different values of X_{J0} and for System 1, System 2, and System 3 (after Marzocchella et al.[33]).

Solid, dashed, and dotted lines report U_1, U'_1, and U_2 as functions of X_{J0}, respectively.

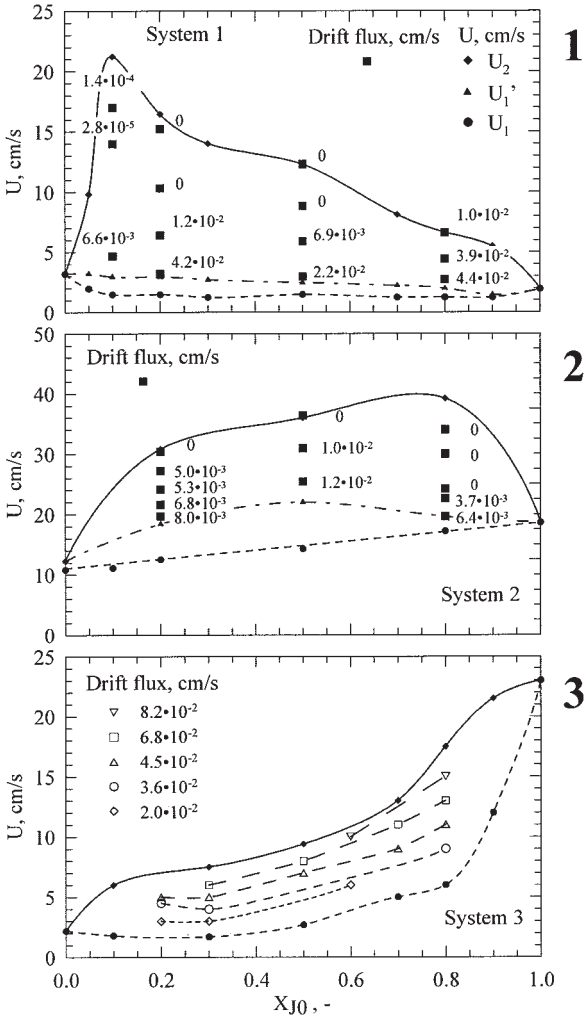

Figure 9. Map of drift flux velocity J_{Jm} for System 1, System 2, and System 3 (after Marzocchella et al.[33]).

mixtures was practically constant (=0.42) with X_{J0} as a consequence of the closeness of particle sizes of the two components (Figure 3.2). The bed voidage of fluidized beds on the verge of bubbling ($U = U_1'$) departs from U_1, especially at small $X_{J,0}$. This behavior was attributed to the occurrence of electrostatic charging of polypropylene particles. Notably, homogeneous bed expansion, which was detected in the single-component bed of pure polypropylene, was emphasized by the addition of silica sand up to $X_{J0} \cong 0.5$. It is speculated that electrostatic forces arising from charge transfer or polarization phenomena might be emphasized when polypropylene was mixed with a limited amount of sand.

Figure 4.2 summarizes results of type A experiments using System 2 mixtures. Gas superficial velocities corresponding to regime transitions are reported as functions of the initial volumetric concentration of the jetsam component X_{J0}. Pronounced maxima in both the U_1' and U_2 curves are observed, whereas U_1 is represented by a straight line connecting the points representative of the pure components.

Results of type B experiments have been worked out for System 2 mixtures similarly to System 1 ones and are reported in Figures 7.2, 8.2, and 9.2. Figure 7.2 shows the mixing index vs. superficial gas velocity for different values of X_{J0}. In Figure 8.2 results are reported as *loci* of the composition of the top layer X_{JT} and of the bottom layer X_{JB} established upon prolonged fluidization at different gas superficial velocities for a given jetsam volumetric fraction. Drift flux velocities are mapped in Figure 9.2. As for System 1 mixtures, a maximum of J_{Jm} is observed at gas superficial velocities close to the lower limit of bubbling transient fluidization U_1'. J_{Jm} becomes vanishingly small as U increases toward U_2.

Discussion

Comparison between the general phenomenology of System 1 and 2 mixtures with that of System 3 mixtures[33] and assessment of segregation parameters are now in order.

Figure 4 highlights similarities and differences between the three systems with respect to fixed/fluidized states of the bed in

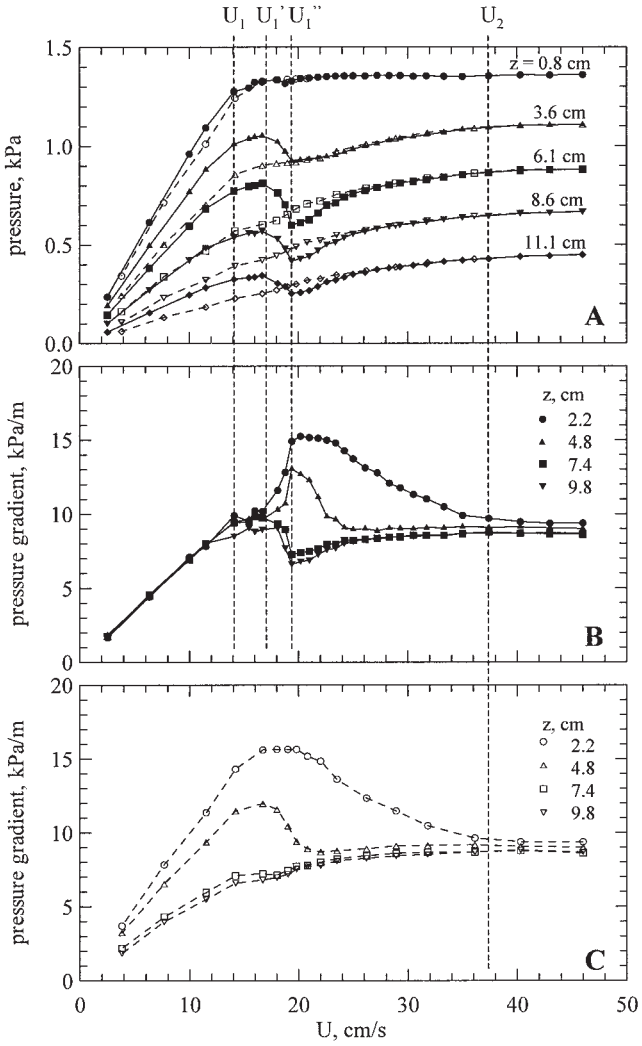

Figure 10. Pressure (A) and pressure gradient (B and C) as functions of gas superficial velocity at different tap locations.

System 2: $X_{J0} = 0.5$. Closed symbols: increasing U; hollow symbols: decreasing U.

the U vs. X_{J0} phase plane. The general sequence of states can be recognized:

(1) Regime I: $U < U_1(X_{J0})$. The granular bed is in the fixed-bed state.

(2) Regime II′: $U_1(X_{J0}) < U < U_1'(X_{J0})$. The bed is in bubble-free fluidized state. Segregation is prevented by the absence of bubbles.

(3) Regime II: $U_1'(X_{J0}) < U < U_2(X_{J0})$. The granular bed is in the transient fluidization regime: the whole bed is fluidized at the beginning, but segregation into jetsam- and flotsam-rich regions occurs thereafter.

(4) Regime III: $U_2(X_{J0}) < U$. The bed is in a bubbling steadily fluidized state. Jetsam composition is uniform throughout the bed.

The existence of Regimes I, II, and III can be recognized, with slightly different features, for all three systems. The rather narrow sub-Regime II′, characterized by bed homogeneous expansion and "metastable" uniform bed composition, is observed with Systems 1 and 2, but not with System 3.

Quantitative assessment of the fluidization/segregation behavior of a binary granular mixture implies the prediction of the limiting values U_1 and U_2.

U_1 is predicted with good accuracy once the value of the static bed voidage of thoroughly mixed solids is known: calculations based on the Carman–Kozeny equation using experimental values of ε (Figure 3) yielded estimates of U_1, which differed from experimental values by less than 5% for all the systems at any X_{J0}. The calculation is particularly simple for System 2, characterized by the property that solids have similar size but different densities. In this case the pressure drop across the fixed bed does not depend on X_{J0}, whereas the minimum velocity at which the pressure drop equals bed weight per unit cross-sectional area[41] is proportional to X_{J0}. Accordingly, U_1 is simply the average between the U_{mf} of both materials weighted by X_{J0}, as suggested by Otero and Corella.[42]

Prediction of the gas velocity at which mixing overtakes segregation—U_2 or the like—as a function of the system properties and of X_{J0} is much more cumbersome. Attempts made along this direction were unsuccessful. Along one path, the empirical correlation proposed by Nienow et al.[43] was considered. This equation, whose validity is restricted to $X_{J0} < 0.5$ and to mixtures of unequal-density components, relates the gas superficial velocity beyond which solids mixing takes over segregation, U_{T0}, to the solids properties and X_{J0}. Values of U_{T0} have been determined for Systems 1 and 2 by working out experimental X_J vs. bed height profiles, and compared with predictions of the Nienow et al.[43] equation. The comparison was unsuccessful. The qualitative and quantitative features of the U_{T0} vs. X_{J0} experimental profiles were poorly reproduced. In particular, the Nienow et al.[43] equation predicts U_{T0} to be a monotonically decreasing function of X_{J0}, a feature not observed in the present study as well as in previous ones.[7] Along a different path, the theoretical framework provided by the Gibilaro and Rowe[23] (G-R) model was considered to analyze the U_2 vs. X_{J0} experimental profiles. The G-R model analyzes the overall segregative flux of one component with respect to the other on the basis of the competing effects of bubble-induced circulation (w, in G-R notation) and segregation (k) fluxes and of axial dispersion (r). If the r term—whose role is essentially that of dictating the sharpness of the interface between the flotsam-rich and the jetsam-rich layers—is neglected, segregation is determined by the balance of w and k terms, expressed through their ratio $\lambda = w/k$. Accordingly, the achievement of the well-mixed condition as $U > U_2$ corresponds to the establishment of large values of λ ($\lambda \gg 1$). Relationships for the prediction of terms appearing in the G-R model, among them λ, were proposed by Naimer et al.[25] Application of these equations, however, does not even reproduce the qualitative features of the U_2 vs. X_{J0} profiles for the systems under investigation. On the whole, it is concluded that theoretical frameworks suitable for quantitative prediction of U_2 as a function of the binary system properties are currently lacking.

It is noteworthy that the different segregation patterns observed in the transient fluidization regime (Regime II) for the three systems can be related to the following features:

- System 3 gives rise mostly to a "fixed-fluidized" segregation pattern: a jetsam-rich bottom layer, in the fixed bed state, and a flotsam-rich top layer, in the fluidized state, coexist.
- Systems 1 and 2 give rise mostly to a "fluidized-fluidized" segregation pattern: a jetsam-rich bottom layer and a flotsam-rich top layer establish upon segregation, both in the fluidized state. As previously recalled, only in a rather narrow range of gas superficial velocities, just beyond U_1', the singularity of a fixed bed of flotsam-rich solids overlaying a jetsam-rich fluidized bottom layer may be observed for System 1.

These discrepancies reflect the different features of maps in Figure 4. The fluidized-fluidized segregation pattern is consistent with the pronounced bell-shaped nature of the U_2 vs. X_{J0} curve of Systems 1 and 2, both characterized by incipient fluidization velocities of the individual components within a factor of 2. In agreement with Hoffmann et al.,[11] the fixed-fluidized segregation pattern is consistent with the lens-shaped, monotonically increasing nature of curves U_1 vs. X_{J0} and U_2 vs. X_{J0}, marking the borderline of the transient fluidization region for System 3. This system is characterized by a substantial difference between the incipient fluidization velocities of the components of the mixture.

The formation of either a fixed or a fluidized bottom layer upon segregation critically affects the extent of axial mixing between the segregated layers, which, in turn, is reflected by the loci $X_{JT}(X_{J0})$ and $X_{JB}(X_{J0})$. When data points in Figure 8 are analyzed in this light, it can be noted that:

- System 3: the loci are substantially overlapped with the boundaries $U_1(X_{J0})$ and $U_2(X_{J0})$ of the transient fluidization region. This implies that System 3 yields top and bottom segregated layers whose jetsam volumetric fractions X_{JT} and X_{JB} are solely determined by the gas superficial velocity, regardless of the composition of the original solids mixture X_{J0}.
- Systems 1 and 2: the loci do not overlap with the limit curves of the transient fluidization regime. The jetsam volume fractions in the top (bottom) layers are always larger (smaller) than those corresponding to the limit curve for any value of the gas superficial velocity. This implies that mixture fractions of top and bottom layers formed by segregation of System 1 and 2 mixtures do depend on the initial mixture fraction X_{J0} in addition to U.

It can be speculated that the establishment of a fixed bed at the bottom during segregation of System 3 mixtures prevents any axial solids mixing between this and the overlaid flotsam-rich layer. On the contrary, the fluidized-fluidized segregation pattern typical of Systems 1 and 2 makes axial mixing between

the two layers effective. This reduces the difference between the mixture fractions of the top and bottom segregated layers to an extent that becomes vanishingly small as the gas superficial velocity approaches U_2. It is likely that the height of the bed, a variable not explored in the context of the present study, might be a critical parameter that affects axial mixing of solids and the actual location of the loci.

The different segregation patterns observed with the three systems is also reflected by the dynamics of solids segregation, expressed by the drift flux velocity J_{Jm}. Analysis of data points in Figure 9 suggests that:

- System 3: the drift flux velocity increases as gas superficial velocity increases, for any given X_{J0}.
- Systems 1 and 2: a maximum in the drift flux velocity is observed close to the lower limit of the transient fluidization regime. The drift flux velocity decreases, becoming vanishingly small, as U increases toward U_2.

When the drift flux data are analyzed in the light of the Gibilaro and Rowe[23] model, the following features can be recognized:

(1) System 3: upflow of solids from the defluidized bottom layer is prevented in this case, and thus $w = \lambda = 0$. Accordingly $J_{Jm} \propto k$, and increases as gas superficial velocity U increases, consistent with experimental findings reported in Figure 9.3.

(2) Systems 1 and 2: upflow of solids and mixing between the layers is permitted in this case, and thus $w \neq 0$. According to Naimer et al.,[25] λ is vanishingly small in the case of very small bubbles, as would be established in shallow beds and/or at small gas superficial velocities, to approach, for a given system, a fairly constant value as the average bubble size is increased. Consistent with this framework, as the gas superficial velocity is increased in the range $U_1 < U < U_2$ both w and k increase, but at a different rate: the circulation flux w increases at a greater rate than k. Accordingly, the net segregative flux J_{Jm} would be a decreasing function of U. Thus, results observed and reported in Figures 9.1 and 9.2 are consistent with the theoretical framework provided by Gibilaro and Rowe[23] and by Naimer et al.[25]

Conclusions

The segregation of fluidized beds consisting of three binary mixtures of solids has been characterized. The extent and the dynamics of solids segregation have been assessed by a combination of experimental procedures. These included time-resolved monitoring of pressures at different levels along the bed and direct characterization of bed material present at various levels of a segmented fluidization column.

The binary systems considered in this study, corresponding to different combinations of particle size and density, were selected in such a way that a broad range of segregation patterns could be covered.

Maps representing the various fixed/fluidized states of the granular beds were built in a gas superficial velocity vs. initial mixture fraction phase plane. A general sequence of fluidization/segregation states emerged by analysis of data relative to the different systems investigated, and four regimes could be identified: fixed-bed regime, bubble-free fluidization regime, transient fluidization regime, and steady fluidization regime. Notably, the shape of the contour of the subdomain corresponding to the transient fluidization regime dictates the phenomenology of segregation. More specifically, this feature determines whether two overlaid fluidized layers ("fluidized-fluidized" segregation pattern) or one fixed/one fluidized layer ("fixed-fluidized" segregation pattern) is generated upon segregation.

Binary systems of components, whose incipient fluidization velocities are close to each other, are characterized by a broad range of gas superficial velocities corresponding to the bubbling transient fluidization regime. Indeed, nonuniform mixture fractions are observed at gas superficial velocities well above the incipient fluidization velocity of the individual components.

The segregation pattern ("fluidized-fluidized" vs. "fixed-fluidized") proved to be extremely influential on the ultimate compositions of the overlaid segregated layers and on the solids segregation rate, expressed by the drift flux velocity. It is speculated that the segregation pattern affects both these properties through the effectiveness of solids mixing between the segregated layers. Differences between the phenomenologies of the various systems investigated could be satisfactorily interpreted, but only on qualitative grounds, in the light of the simple mechanistic framework provided by the Gibilaro and Rowe model.[23]

The incipient fluidization velocities of the well-mixed binary systems were accurately predicted by the Carman–Kozeny equation using the experimentally determined values of the fixed-bed voidage. On the contrary, quantitative prediction of the gas velocity at which solids mixing takes over segregation was unsatisfactory: both the Nienow et al.[43] equation and the mechanistic segregation model developed by Gibilaro and Rowe[23] could not reproduce experimental data.

Generalization of results obtained within the present work to other systems is still an open issue because of the complexity of the systems at hand and the current lack of mechanistic understanding of phenomena underlying segregation. Questions that are still largely unresolved regard: the interplay of particle size and density differences between the components as the driving forces of segregation (the minimum fluidization velocity of the individual components proves not to be an adequate scaling parameter); the quantitative prediction of the gas superficial velocity beyond which uniform composition of the bed is established; and the quantitative prediction of the drift flux velocity.

Acknowledgments

Financial support from MIUR within the framework of the research program on "Multiphase systems for granular solids processing and heterogeneous reaction in the process industry" is acknowledged.

Notation

A = cross-sectional area of the fluid bed, m^2
g = acceleration attributed to gravity, m/s^2
H = bed height, cm
H^* = static bed height under fully segregated conditions, cm
k = segregation flux, cm/s
J_{Jm} = drift flux velocity, cm/s
M = mixing index
P = pressure, kPa
r = axial mixing coefficient, cm^2/s
t = time, s
U = superficial gas velocity, cm/s

U_1, U_1', U_2 = superficial gas velocity at the threshold of the fluidization regimes, cm/s
U_1'' = superficial gas velocity corresponding to maximum segregation, cm/s
U_{mf} = minimum fluidization velocity, cm/s
w = circulation flux, cm/s
W_{bed} = total weight of the bed material, kg
X_J = volumetric fraction of jetsam particles
X_J^* = volumetric fraction of jetsam particles under fully segregated conditions
X_J = average volume fraction of jetsam in the solids mixture
X_{JT}, X_{JB} = volumetric fraction of jetsam particles in the top/bottom segregated layers
z = axial bed coordinate, m

Greek letters

ε = voidage
λ = parameter of Gibilaro and Rowe[23] model
ρ = density, kg/m^3

Subscripts

b = bed
F = flotsam particle
J = jetsam particle
s = solid

Literature Cited

1. Gel'perin NI, Ainshtein VG, Kvasha VB, Kogan AS, Vil'nits SA. Apparatus for classification of free-flowing materials in a fluidized bed. *International Chemical Engineering.* 1964;4:198-203.
2. Nienow AW, Chiba T. Fluidization of dissimilar materials. In: Davidson JF, Clift R, Harrison D, eds. *Fluidization* (2nd edition). London: Academic Press; 1985:357-382.
3. Fan LT, Chen YM, Lai FS. Recent development in solids mixing. *Powder Technology.* 1990;61:255-287.
4. Mourad M, Hemati M, Laguerie C. Hydrodynamique d'un séchoir à lit fluidisé à flottation: Détermination des vitesses caractéristiques de fluidisation de mélanges de mais et de sable. *Powder Technology.* 1994;80:45-54.
5. Dolgunin VN, Ukolov AA. Segregation model of particle rapid gravity flow. *Powder Technology.* 1995;83:95-103.
6. Khang DY, Lee HH. Particle size distribution in fluidized beds for catalytic polymerization. *Chemical Engineering Science.* 1997;52:421-431.
7. Yang WC, Keairns DL. Rate of particle separation in a gas fluidized bed. *Industrial and Engineering Chemistry Fundamentals.* 1982;21: 228-235.
8. Thonglimp V, Hiquily N, Laguarie C. Minimal velocity of fluidization and expansion of layers of gas-fluidised mixtures of solid particle. *Powder Technology.* 1984;39:223-239.
9. Noda K, Uchida S, Makino T, Kamo H. Minimum fluidization velocity of binary mixture of particles with large size ratio. *Powder Technology.* 1986;46:149-154.
10. Formisani B. Packing and fluidization properties of binary mixtures of spherical particles. *Powder Technology.* 1991;66:259-264.
11. Hoffmann AC, Janssen LBPM, Prins J. Particle segregation in fluidized binary mixtures. *Chemical Engineering Science.* 1993;48:1583-1592.
12. Rasul MG, Rudolph V, Carsky M. Segregation potential in binary gas fluidized beds. *Powder Technology.* 1999;103:175-181.
13. Formisani B, De Cristofaro G, Girimonte R. A fundamental approach to the phenomenology of fluidization of size segregating binary mixtures of solids. *Chemical Engineering Science.* 2001;56:109-119.
14. Gilbertson MA, Eames I. Segregation patterns in gas-fluidized systems. *Journal of Fluid Mechanics.* 2001;433:347-356.
15. Yang WC, Keairns DL. Further studies on the rate of particle separation in gas-fluidized bed. *Journal of Chinese Institute of Chemical Engineering.* 1991;22:419-426.
16. Garcìa-Ochoa F, Romero A, Villar JC, Bello A. A study of segregation in a gas-solid fluidized bed: Particles of different density. *Powder Technology.* 1989;58:169-174.
17. Hemati M, Spieker K, Laguerie C, Alvarez R, Riera FA. Experimental study of sawdust and coal particles mixing in sand or catalyst fluidized beds. *Canadian Journal of Chemical Engineering.* 1990;68:768-772.
18. Kozanoglu B, Levy EK. Mixing dynamics in a bubbling fluidized bed with binary solids. In: Owen OE, Nicklin DJ, eds. *Fluidization VII.* New York, NY: Engineering Foundation; 1992:141-149.
19. Beeckmans JM, Agarwal R. Studies on transport processes in a segregating fluidised bed. *Powder Technology.* 1994;80:17-23.
20. Hoomans BPB, Kuipers JAM, Briels WJ, van Swaaij WPM. Discrete particle simulation of segregation phenomena in dense gas-fluidized beds. In: Fan LS, Knowlton T, eds. *Fluidization IX*. New York, NY: Engineering Foundation; 1998:485-492.
21. Zhang JY, Luo GH, Pen H. High efficiency segregation of particles in gas fluidized beds. In: Fan LS, Knowlton T, eds. *Fluidization IX*. New York, NY: Engineering Foundation; 1998:717-724.
22. Wu SY, Baeyens J. Segregation by size difference in gas fluidised bed. *Powder Technology.* 1998;98:139-150.
23. Gibilaro LG, Rowe PN. A model for a segregating gas fluidised bed. *Chemical Engineering Science.* 1974;29:1403-1412.
24. Rowe PN, Nienow AW. Particle mixing and segregation in gas fluidized beds. A review. *Powder Technology.* 1976;15:141-147.
25. Naimer NS, Chiba T, Nienow WA. Parameter estimation for a solids mixing/segregation model for gas fluidised beds. *Chemical Engineering Science.* 1982;37:1047-1057.
26. Valkenburg PJM, Schouten JC, van den Bleek CM. The non-steady state segregation of particles in gas fluidized beds. In: Ostregaard K, Sorensen A, eds. *Fluidization V*. New York, NY: United Engineering Trustees; 1986:193-200.
27. Kim JY, Choi KY. Polymer particle mixing and segregation in a gas phase olefin polymerization reactor. *AIChE Symposium. Series.* 1999; 95:77-82.
28. Bilbao R, Lezaun J, Mendez M, Izquierdo MT. Segregation in straw/sand mixture in fluidised bed in unsteady state. *Powder Technology.* 1991;68:31-35.
29. Hoomans BPB, Kuipers JAM, van Swaaij WPM. Granular dynamics of segregation phenomena in bubbling gas-fluidised beds. *Powder Technology.* 2000;109:41-48.
30. Van Wachem BGM, Schouten JC, van den Bleek CM, Krishna R, Sinclair JL. CFD modeling of gas-fluidised beds with a bimodal particle mixture. *AIChE Journal.* 2001;47:1292-1302.
31. Huilin L, Yurong H, Gidaspow D, Lidan Y, Yukun Q. Size segregation of binary mixture of solids in bubbling fluidized beds. *Powder Technology.* 2003;134:86-97.
32. Marzocchella A, Salatino P, Di Pastena V, Lirer L. Fluidization in pyroclastic flow. In: Fan LS, Knowlton T, eds. *Fluidization IX*. New York, NY: Engineering Foundation; 1998:389-396.
33. Marzocchella A, Salatino P, Di Pastena V, Lirer L. Transient fluidization and segregation by size difference of binary mixtures of particles. *AIChE Journal.* 2000;46:2175-2182.
34. Di Pastena V. Aspetti fluidodinamici dei flussi piroclastici. PhD Thesis, Università degli Studi di Napoli Federico II, Naples, Italy; 1997.
35. Haider A, Levenspiel O. Drag coefficient and terminal velocity of spherical and nonspherical particles. *Powder Technology.* 1989;58:63-70.
36. Chiba S, Nienow AW, Chiba T, Kobayashi H. Fluidised binary mixtures in which the denser component may be flotsam. *Powder Technology.* 1980;26:1-10.
37. D'Amore M, Donsì G, Massimilla L. The influence of bed moisture of fluidization characteristic of fine powders. *Powder Technology.* 1979; 23:253-259.
38. Massimilla L, Donsì G, Zucchini C. The structure of bubble-free gas fluidized beds of fine fluid cracking catalyst particles. *Chemical Engineering Science.* 1972;27:2005-2015.
39. Donsì G, Massimilla L. Bubble-free expansion of gas fluidized beds of fine particles. *AIChE Journal.* 1973;19:1104-1110.
40. Kunii D, Levenspiel O. *Fluidization Engineering*. New York: NY: Wiley; 1969.
41. Couderc JP. Incipient fluidization and particulate systems. In: Davidson JF, Clift R, Harrison D, eds. *Fluidization* (2nd edition). London: Academic Press; 1985:1-46.
42. Otero AR, Corella J. *Anales de la Real Sociedad Española de Física y Química.* 1971;B67:1207-1212.

43. Nienow AW, Rowe PN, Cheung LYL. A quantitative analysis of the mixing of two segregating powders of different density in a gas-fluidised bed. *Powder Technology.* 1978;20:89-97.

Appendix: Procedure for the Calculation of the Drift Flux Velocity

The local mass balance on the jetsam component is expressed as

$$\frac{\partial J_{Jm}}{\partial z} = -\frac{\partial X_J}{\partial t} \tag{A1}$$

where J_{Jm} is the axial drift flux velocity and z is an axial coordinate whose origin is located at the base of the fluidized bed. By integration of Eq. A1 between z and the bed height (where the drift flux is equal to zero) one obtains

$$J_{Jm} = \int_z^H \frac{\partial X_J}{\partial t} \cdot dz \tag{A2}$$

The pressure at the coordinate z within a fluidized bed of a binary mixture is given by

$$P = \int_z^H [\rho_J X_J + \rho_F(1 - X_J)](1 - \varepsilon)\, g dz \tag{A3}$$

On the hypothesis that H and ε are constant during the experiment, the time derivative of pressure is

$$\frac{\partial P}{\partial t} = (\rho_J - \rho_F)(1 - \varepsilon)\, g \int_z^H \frac{\partial X_J}{\partial t}\, dz \tag{A4}$$

By combining Eqs. A1 and A4, one obtains

$$J_{Jm} = \frac{1}{(\rho_J - \rho_F)(1 - \varepsilon)\, g} \frac{\partial P}{\partial t} \tag{A5}$$

which provides a relationship between the drift flux across a given bed section and the time derivative of pressure. The latter is computed by working out the pressure time series recorded at the specified level in the bed.

Manuscript received Apr. 10, 2003, revision received Mar. 31, 2004, and final revision received July 5, 2004.